Journal of
Materials Chemistry B

Accepted Manuscript

This article can be cited before page numbers have been issued, to do this please use: X. Ma and P. Miao, *J. Mater. Chem. B*, 2019, DOI: 10.1039/C9TB00274J.

ROYAL SOCIETY OF CHEMISTRY

rsc.li/materials-b

View Article Online
DOI: 10.1039/C9TB00274J

Journal

COMMUNICATION

Silver nanoparticle@DNA tetrahedron based colorimetric detection of HIV-related DNA with cascade strand displacement amplification†

Received 00th January 20xx,
Accepted 00th January 20xx

DOI: 10.1039/x0xx00000x

www.rsc.org/

Xiaoyi Ma,[ab] and Peng Miao*[ab]

DNA tetrahedrons modified silver nanoparticles (AgNPs) are achieved via amino-silver chemistry for the first time, which are applied in a colorimetric biosensor for detecting HIV-related DNA. Target DNA initiated strand displacement polymerization and nicking endonuclease aided cycles are involved to link DNA tetrahedron modified AgNPs, reporting colorimetric responses. This developed method shows excellent specificity and sensitivity. A wide linear range from 1 to 15000 nM is achieved with a limit of detection of 0.84 nM. Moreover, it has been successfully applied to determine DNA in blood serum samples.

Acquired deficiency syndrome (AIDS) is a tremendously lethal infectious disease induced by human immunodeficiency virus (HIV), which destroys the immune system of human beings.[1] HIV is a kind of RNA virus which owns two RNA chains in the genome.[2] CD4 lymphocytes are the main targets in the immune system for attacking.[3] After invaded in host cells, RNA will be transcribed into DNA for further gene expression. AIDS patients are susceptible to various diseases and malignant tumors may be developed. The mortality rate of AIDS is extremely high. Therefore, there are urgent needs to develop accurate and convenient methods for the detection HIV-related DNA for the purposes of early diagnosis and clinical therapy of AIDS.[4]

Currently, a number of traditional techniques have been applied for DNA detection such as flow cytometry, northern blotting analysis, microarray and so on. However, these methods cannot meet the requirements of point-of-care (POC) testing due to the requirements for skilled operation, expensive equipment, complicated reagents and time-consuming procedures. Development of novel biosensors is much essential. During the past years, a diversity of DNA assay methods have been proposed utilizing techniques including fluorescence,[5-6] chemiluminescence,[7-9] electrochemistry,[10] photoelectrochemistry[11] nanopore-based assay,[12] and colorimetry.[13] Among them, colorimetry has attracted extensive attention due to its easy operation, low cost, and intuitive display.[14] Gold nanoparticles (AuNPs) and silver nanoparticles (AgNPs) show wonderful localized surface plasmon resonance (LSPR) properties, which are excellent materials for colorimetric biosensors.[15] The colors of the colloidal systems always rely on their sizes, morphologies, capping molecules, and distribution states. AgNPs are gaining more and more attention since they possess higher extinction coefficients, facile synthesis and functionalization properties.[16-17]

However, the sensitivity of colorimetric sensor is always limited, which requires the involvement of signal amplification. So far, a diversity of amplification strategies have been adopted in biosensors. PCR is the most widely used technique with well-behaved sensitivity. To simplify the testing system, isothermal reactions are excellent alternatives, such as rolling circle amplification (RCA),[18] exonuclease aided target recycling,[19] "click" chemistry,[20] hybridization chain reaction (HCR),[21] strand displacement amplification (SDA),[22] and catalyzed-hairpin-assembly (CHA) amplification.[23] Furthermore, polymerization/nicking machinery always achieves higher sensitivity with cascade amplification.[24-25] For instance, Willner's group developed an autonomous isothermal DNA biosensor with replication/nicking processes and the displacement of a DNAzyme to generate the emission of fluorophore.[26] Similarly, Ye's group also coupled DNA polymerase with nicking endonuclease for amplified detection of RNA in complex biological samples.[27] The generated products opened the molecular beacon for fluorescence readout. Ge et al. designed a label-free homogeneous electrochemical system to achieve DNA logic gates by the employment of polymerization/nicking machines.[28] Qu et al. performed strand displacement polymerization and nicking reactions on quantum dot-encoded silica bead for visual analysis of RNA.[29] Huang et al. designed a graphene oxide-based fluorescent biosensor platform with target-induced polymerization/nicking reactions for signal amplification.[30]

[a] University of Science and Technology of China, Hefei 230026, China
*E-mail: miaopeng@sibet.ac.cn; Fax: +86-512-69588283
[b] Suzhou Institute of Biomedical Engineering and Technology, Chinese Academy of Sciences, Suzhou, China

† Electronic Supplementary Information (ESI) available: [Fig. S1-4, Table S1-2]. See DOI: 10.1039/x0xx00000x

View Article Online
DOI: 10.1039/C9TB00271J

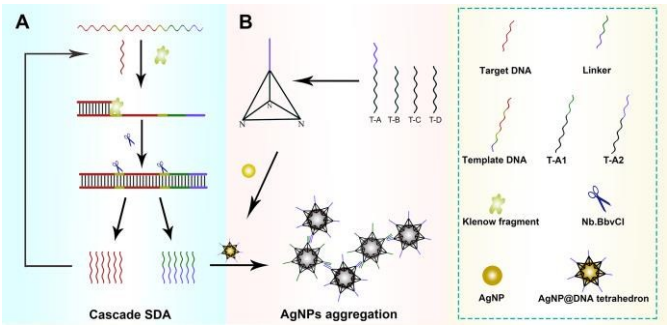

Scheme 1. Illustration of (A) Target DNA-induced cascade strand displacement amplification; (B) AgNP@DNA tetrahedron based colloid system for sensitive detection of DNA.

In this work, we have integrated the advantages of colorimetric system and polymerization/nicking machinery. An amplified colorimetric biosensor for the detection of HIV-related DNA is proposed. After target-triggered reactions, numerous DNA strands are produced, which can be used to link DNA tetrahedron modified AgNPs for colorimetric responses. This method shows excellent analytical performances due to the strand displacement polymerization and nicking endonuclease aided cycles. It can also be facilely operated and the colloid system is much stable with DNA tetrahedron modification. Moreover, mismatched DNAs can be successfully distinguished. Therefore, this method may provide great potential in the biomedical researches and clinical diagnosis.

Detailed working strategy is shown in Scheme 1. Generally, a single-stranded Template DNA is designed which contains complementary sequence of Linker DNA, two target recognition regions, and two restriction sites of Nb.BbvCI. Target DNA works as a primer, which partially hybridizes with Template DNA, and is able to be extended by Klenow fragment polymerase. The formed complete double-stranded DNA can be cleaved by Nb.BbvCI, producing two nicks. With continuous polymerase-catalyzed reaction, Target DNA and Linker DNA probes are displaced. The released Target DNA can be further used for more cycles of hybridization, extension, nicking and strand displacement reactions. Compared with conventional polymerization/nicking machinery, two target recognition regions are designed and the efficiency of target recycling is improved significantly. Therefore, numerous Linker DNA probes are produced by the cascade SDA. On the other hand, the distribution state of AgNP@DNA tetrahedron is controlled as colorimetric response of this DNA biosensor. DNA tetrahedrons are firstly formed by four single-stranded DNA probes, which can be characterized by polyacrylamide gel electrophoresis. In the gel image, DNA structures formed by one, two, three and four strands are clearly shown and their molecular weights are in good agreement with expected values (Fig. S1). Since the probes of T-B, T-C and T-D are modified with amino groups at the 5' terminals, the formed DNA tetrahedrons contain three amino vertices, which facilitate their immobilization on the surface of AgNPs via amino-silver chemistry.[31] This three-dimensional immobilization mode shows several advantages over traditional single-stranded or hairpin-structured immobilization modes. First, three functional groups at the bottom of DNA tetrahedron make the conjugation more stable.[32] Second, functionalization of single-stranded DNA on the surface of nanoparticles always requires a "salt-aging" process, which is quite time-consuming.[33-35] It can be eliminated in the case of DNA tetrahedron functionalization. Third, the proposed DNA immobilization mode provides more efficiency of accessibility and hybridization.[36-38] Since the two single-stranded sequences on top of the two DNA tetrahedron can partially hybridize with Linker DNA, remarkable aggregation of AgNPs occurs with plenty of Linker DNA produced by the cascade SDA. In addition, in the DNA nanostructure formed by Linker DNA and DNA tetrahedrons, Linker DNA is folded, which is different from traditional sandwich structure. This design shortens the distance between two AgNPs for enhanced LSPR effect. Finally, by studying UV-vis absorption spectra of AgNPs, sensitive analysis of Target DNA is achieved.

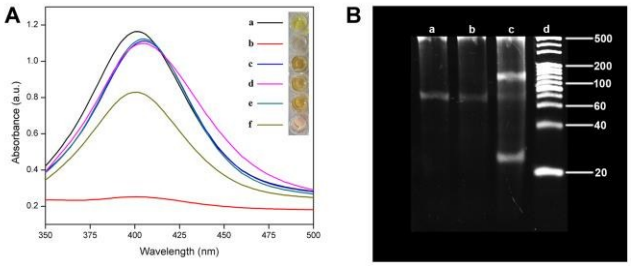

Fig. 1 (A) UV-vis absorption spectra of (a) bare AgNPs, (b) AgNPs with salt, (c) AgNP@DNA tetrahedron, (d) AgNP@DNA tetrahedron with salt, AgNP@DNA tetrahedron colloid systems with salt after SDA in the (e) absence and (f) presence of Target DNA. (B) Gel electrophoresis image for different nucleic acids samples: (a) Template DNA, (b) Template DNA after SDA in the absence of Target DNA, (c) Template DNA after SDA in the presence of Target DNA.

The sensing strategy for Target DNA assay can be directly proved by the observation of the distribution states of AgNP@DNA tetrahedron by transmission electron microscope (TEM). The size of the nanocomposites is estimated to be 5 to 10 nm, which is well-dispersed in the solution containing salt with high concentration (Fig. S2). However, after Target DNA initiated cascade SDA, numerous Linker DNA are produced and obvious crosslinking aggregation of AgNPs is thus observed (Inset in Fig. S2). More evidences can be obtained by observing UV-vis absorption spectra or even the solution colors. As shown in Fig. 1A, a significant peak appears at 400 nm for bare AgNP (curve a). However, after the addition of certain salt, the peak disappears, indicating the salt-induced aggregation of unprotected AgNPs (curve b). However, the peak at 400 nm barely changes for AgNP@DNA tetrahedron even with the addition of salt, which is owing to the DNA protection effect (curve c and d). In the absence of Target DNA, no Linker DNA is supposed to be produced, thus the UV-vis absorption spectrum is also unaltered (curve e). However, after Target DNA-triggered SDA, plenty of Linker DNA probes are generated, which lead to crosslinking aggregation of AgNP@DNA tetrahedrons. Thus, the peak at 400 nm drops significantly (curve f). By observing color variations of corresponding colloid systems, similar conclusions can also be obtained (Inset in Fig.

1A). To confirm the reactions of DNA hybridization, extension, nicking and strand displacement, gel electrophoresis is performed. As shown in Fig. 1B, a bright band is shown in lane a, which is ascribed to Template DNA. In the absence of Target DNA, SDA cannot occur, thus the position of DNA band is not changed (lane b). After hybridized with Target DNA and further SDA reactions, complete double-stranded DNA and displaced single-stranded DNA are observed (lane c). The gel experiments have well demonstrated the SDA reactions.

In order to achieve DNA assay with high sensitivity, we have performed more experiments to optimize the reaction conditions (Fig. S3). Linker DNA is synthesized and added to the AgNP@DNA tetrahedrons with different time durations. The UV-vis absorption peak gradually decreases, and keeps stable after 90 min. Thereby, 90 min is used for AgNPs incubation in the following experiments. Different concentrations of enzymes are also tested. With more enzymes, much obvious peak changes are produced. Considering the reaction efficiency and cost, 0.3 U/μL Nb.BbvCI and 0.06 U/μL Klenow fragment polymerase are chosen for SDA. The reaction temperature is also an important parameter for enzymatic reactions. After comparing the UV-vis absorption responses in the cases of 20°C, 25°C, 30°C, 37°C, the optimized temperature of 30°C is selected.

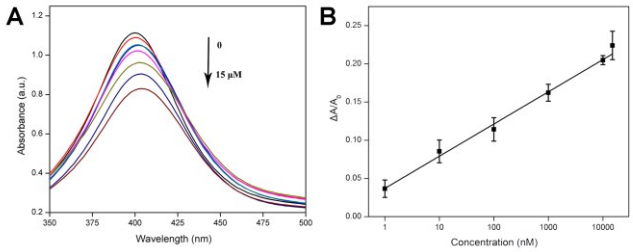

Fig. 2 (A) UV-vis absorption spectra of AgNP@DNA tetrahedron based colorimetric biosensor for the detection of DNA with the concentrations of 0, 10^{-9}, 10^{-8}, 10^{-7}, 10^{-6}, 10^{-5}, 1.5×10^{-5} M (from top to bottom). (B) Calibration plot reflecting the relationship between logarithmic DNA concentration and $\Delta A/A_0$. Error bars represent the standard deviations of three independent measurements.

UV-vis absorption spectra for the detection of different concentrations of DNA are recorded to disclose the relationship between Target DNA concentration and distribution states of the colloidal system. As shown in Fig. 2A, with the increase of Target DNA level, the peak drops gradually. Since the absorbance value at 400 nm represents the degree of the aggregation of AgNPs. We have then studied the relationship between $\Delta A/A_0$ (A_0 stands for absorbance at 400 nm without target, ΔA represents decreased absorbance at 400 nm in the presence of Target DNA compared with A_0) and the concentration of Target DNA. A linear relationship is established from 1 nM to 15 μM, which is quite wide (Fig. 2B). The equation is as follows:

$$y = 0.04214\,x + 0.03695 \quad (n = 3,\ R^2 = 0.99564)$$

in which, y stands for the reduction ratio of absorbance value at 400 nm, x is the logarithm of concentration of Target DNA (nM). The limit of detection is calculated to be 0.84 nM. Although the analytical performances are not better than polymerization/nicking machinery-based fluorescent sensors, the proposed method omits the use of sophisticated instrument which may have better potential practical utility. In addition, it is found that this method is more sensitive than most reported colorimetric methods (Table S1). Moreover, the formed AgNP@DNA tetrahedron shows high stability owing to the protection of DNA nanostructures. After stored for 1 month, the color of the colloid system is unchanged with uniform UV-vis absorption peak at 400 nm.

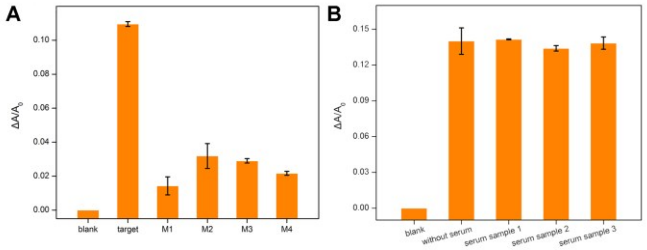

Fig. 3 (A) Selectivity investigation of the colorimetric assays to distinguish mismatched DNA (100 nM) by comparing corresponding values $\Delta A/A_0$. (B) Detection of Target DNA in serum samples. The spiked Target DNA concentration is 1 μM. Error bars represent the standard deviations of three independent measurements.

To investigate the selectivity of this method, we have displaced Target DNA by four mismatched DNA strands. The absorbance peaks at 400 nm are close to the blank curve. While Target DNA triggers SDA and produces numerous Linker DNA for AgNPs aggregation, the variation of absorbance value at 400 nm is relatively large (Fig. 3A), demonstrating the high selectivity of the method. To verify the practical application of this method, Target DNA is firstly spiked in the human serum samples, the levels of which are then detected by the proposed method. We have compared the values of $\Delta A/A_0$. The results listed in Fig. 3B show excellent consistence with that in buffered solution, demonstrating that the proposed method is applicable in complicated biological samples.

Conclusions

In summary, we have developed a novel colorimetric biosensor for sensitive and selective detection of HIV-related DNA, which shows remarkable merits. First, we have achieved DNA tetrahedron modified AgNPs via amino-silver chemistry for the first time. This structure helps increase DNA probe reactivity and accessibility, which is superior to single-stranded or hairpin-structured DNA modified AgNPs. Second, Target DNA induces multiple strand displacement polymerization reactions, which are aided by nicking endonuclease. The enzymatic combination contributes to cascade signal amplification and sub-nanomolar sensitivity is achieved. Furthermore, the application of this AgNP@DNA tetrahedron colloid system is successfully applied for DNA assay in complicated biological samples. Therefore, this work may have great potential utility for biomedical searches and clinical diagnosis in near future.

This work is supported by the National Natural Science Foundation of China (Grant No. 81771929), the Key R&D Program of Tianjin (Grant No. 18YFZCSY01290), and the Scientific Research Instrument Developing Project of the Chinese Academy of Sciences (Grant No. YJKYYQ20170067).

Experimental

Materials and instruments

Sodium chloride (NaCl), sodium dihydrogen phosphate (NaH_2PO_4), dibasic sodium phosphate (Na_2HPO_4) were purchased from Aladdin Biological Technology Co., Ltd. (Shanghai, China). Tris (2-carboxyethyl) phosphine (TCEP), sodium borohydride ($NaBH_4$), trisodium citrate, and ethylenediaminetetraacetic acid (EDTA) were obtained from Sigma (USA). Silver nitrate ($AgNO_3$) was from Shanghai Jiushan Chemicals Co., Ltd. (Shanghai, China). All DNA sequence and 4S Red Plus were from Sangon Biotechnology Co. Ltd. (Shanghai, China). Klenow fragment polymerase, Nb.BbvCI nicking endonuclease, dNTPs and CutSmart buffer were purchased from New England Biolabs (Beijing, China). 20 bp DNA Ladder was obtained from Takara Biotechnology Co., Ltd. (Dalian, China). All other chemicals were of analytical grade without further purification. Water used in this work was purified by a Millipore water purification system with a specific resistance of 18 MΩ·cm. UV-vis absorption spectra were measured by Synergy HT multifunction microplate reader (BioTek Instruments, Inc., USA). Polyacrylamide gel was photographed under UV light by GelDoc XR$^+$ System (Bio-Rad, USA). Transmission electron microscopic (TEM) images were taken by a FEI Tecnai G20 transmission electron microscopy (FEI, USA).

Preparation of AgNP@DNA tetrahedron

Bare AgNPs were synthesized by the borohydride reduction of $AgNO_3$ according to a previous report.[39] Briefly, $AgNO_3$ and trisodium citrate solution with independent concentrations of 0.25 mM was firstly prepared. Next, 100 mL of the solution was blended with 3 mL of $NaBH_4$ solution with the concentration of 10 mM. After intense stirring for half an hour, the solution was stood still overnight in the dark. AgNPs with bright yellow color were then synthesized. The AgNPs were further purified by three cycles of centrifugation at 14,000 rpm for 20 min. Then, AgNPs were resuspended with the concentration of 8 nM.

DNA tetrahedron was self-assembled by simply mixing four single-stranded DNA strands.[40] Two independent tetrahedrons were formed using two groups of DNA probes (T-A1, T-B, T-C, T-D; T-A2, T-B, T-C, T-D). Generally, four DNA strands with the concentrations of 100 μM were prepared with hybridization buffer (10 mM phosphate buffer with 0.2 M NaCl, pH 7.4), respectively. 2 μL of each strand was added into 192 μL of hybridization buffer. The mixture was heated to 95℃ for 5 min and then cooled to room temperature gradually. The formed DNA nanostructure was then mixed with AgNPs with the ratio of 1 : 9. After reacted overnight at room temperature, DNA tetrahedron could be modified on the surface of AgNPs via amino-silver chemistry. Afterward, two nanocomposites (AgNP@DNA tetraheron-1 and AgNP@DNA tetraheron-2) were purified by centrifugation at 14, 000 rpm for 60 min, respectively.

In order to calculate the DNA tetrahedron density on AgNPs, a calibration plot reflecting the relationship between DNA tetrahedron concentration and OD260 was established (Fig. S4). After the incubation of DNA tetrahedron with AgNPs with the ratio of 1 : 9, the nanoconjugates were centrifuged and OD260 of the supernatant liquid was measured (0.087). By comparing with the equation in Fig. S4, the amount of unconjugated DNA tetrahedron in the supernatant liquid could be obtained, which accounted for three-tenth of original DNA tetrahedron level. As a result, the average number of DNA tetrahedrons on each AgNP was estimated to be 8 to 9.

View Article Online DOI: 10.1039/C9TB00274J

Colorimetric assay with cascade signal amplification

A series of concentrations of Target DNA were prepared. After that, they were added to the CutSmart buffer (20 mM Tris-acetate, 10 mM magnesium acetate, 50 mM potassium acetate, 100 μg/mL BSA, pH 7.9) containing 5 μM Template DNA, 250 μM dNTPs, 0.3 U/μL Nb.BbvCI and 0.06 U/μL Klenow fragment polymerase. The solutions (50 μL) reacted at 30℃ for 90 min. Subsequently, they were heated to 85℃ for 20 min so as to terminate the reactions. After cooled to room temperature, 75 μL of AgNP@DNA tetraheron-1 and 75 μL of AgNP@DNA tetraheron-2 were added. The mixtures were placed in 96-well plate and were incubated at room temperature for 90 min. UV-vis absorption spectra were then recorded. The absorbance values at 400 nm (A_{400nm}) were obtained which were related to the concentration of Target DNA.

Interference investigation and real sample analysis

To verify the selectivity of this method, four DNA probes with similar sequences were employed instead of Target DNA. After SDA reactions in the presence of mismatched DNAs (100 nM), UV-vis absorption spectra were measured. To examine the utility of this strategy in complicated biological samples, three independent human serum samples were collected and diluted for 10 times. Afterward, Target DNA (1 μM) was spiked into these samples. The mixtures were directly challenged with the proposed colorimetric biosensor.

Notes and references

1. X. L. Wu, T. Q. Zhou, J. Zhu, B. S. Zhang, I. Georgiev, C. Wang, X. J. Chen, N. S. Longo, M. Louder, K. McKee, S. O'Dell, S. Perfetto, S. D. Schmidt, W. Shi, L. Wu, Y. P. Yang, Z. Y. Yang, Z. J. Yang, Z. H. Zhang, M. Bonsignori, J. A. Crump, S. H. Kapiga, N. E. Sam, B. F. Haynes, M. Simek, D. R. Burton, W. C. Koff, N. A. Doria-Rose, M. Connors, J. C. Mullikin, G. J. Nabel, M. Roederer, L. Shapiro, P. D. Kwong, J. R. Mascola and N. C. S. Progra, *Science*, 2011, **333**, 1593-1602.

2. S. C. Keane, X. Heng, K. Lu, S. Kharytonchyk, V. Ramakrishnan, G. Carter, S. Barton, A. Hosic, A. Florwick, J. Santos, N. C. Bolden, S. McCowin, D. A. Case, B. A. Johnson, M. Salemi, A. Telesnitsky and M. F. Summers, *Science*, 2015, **348**, 917-921.

3. D. D. Ho, A. U. Neumann, A. S. Perelson, W. Chen, J. M. Leonard and M. Markowitz, *Nature*, 1995, **373**, 123-126.

4. B. Y. Fang, C. Li, J. An, S. D. Zhao, Z. Y. Zhuang, Y. D. Zhao and Y. X. Zhang, *Nanoscale*, 2018, **10**, 5532-5538.

5. X. L. Zuo, F. Xia, Y. Xiao and K. W. Plaxco, *J. Am. Chem. Soc.*, 2010, **132**, 1816-1818.

6. S. Z. Yue, T. T. Zhao, H. J. Qi, Y. C. Yan and S. Bi, *Biosens. Bioelectron.*, 2017, **94**, 671-676.
7. R. Freeman, X. Q. Liu and I. Willner, *J. Am. Chem. Soc.*, 2011, **133**, 11597-11604.
8. H. J. Qi, S. Z. Yue, S. Bi, W. L. Song and C. F. Ding, *Sens. Actuator B-Chem.*, 2018, **273**, 1525-1531.
9. Y. C. Yan, S. Z. Yue, T. T. Zhao, B. Y. Luo and S. Bi, *Chem. Commun.*, 2017, **53**, 12201-12204.
10. B. Li, G. H. Pan, N. D. Avent, R. B. Lowry, T. E. Madgett and P. L. Waines, *Biosens. Bioelectron.*, 2015, **72**, 313-319.
11. W. Lu, Y. Jin, G. Wang, D. Chen and J. H. Li, *Biosens. Bioelectron.*, 2008, **23**, 1534-1539.
12. Y. Wang, K. Tian, X. Du, R. C. Shi and L. Q. Gu, *Anal. Chem.*, 2017, **89**, 13039-13043.
13. F. Xia, X. L. Zuo, R. Q. Yang, Y. Xiao, D. Kang, A. Vallee-Belisle, X. Gong, J. D. Yuen, B. B. Y. Hsu, A. J. Heeger and K. W. Plaxco, *Proc. Natl. Acad. Sci. U. S. A.*, 2010, **107**, 10837-10841.
14. L. M. Wei, X. Y. Wang, D. Wu, C. Li, Y. M. Yin and G. X. Li, *Chem. Commun.*, 2016, **52**, 5633-5636.
15. Y. Cao, J. Wang, Y. Y. Xu and G. X. Li, *Biosens. Bioelectron.*, 2010, **25**, 1032-1036.
16. Y. Liu and C. Z. Huang, *Analyst*, 2012, **137**, 3434-3436.
17. P. Miao, Y. G. Tang and J. Yin, *Chem. Commun.*, 2015, **51**, 15629-15632.
18. F. Wang, C. H. Lu, X. Q. Liu, L. Freage and I. Willner, *Anal. Chem.*, 2014, **86**, 1614-1621.
19. X. J. Liu, W. Li, T. Hou, S. S. Dong, G. H. Yu and F. Li, *Anal. Chem.*, 2015, **87**, 4030-4036.
20. Y. Zou, L. Zhang, L. Yang, F. Zhu, M. M. Ding, F. Lin, Z. Wang and Y. W. Li, *J. Control. Release*, 2018, **273**, 160-179.
21. Z. L. Ge, M. H. Lin, P. Wang, H. Pei, J. Yan, J. Y. Sho, Q. Huang, D. N. He, C. H. Fan and X. L. Zuo, *Anal. Chem.*, 2014, **86**, 2124-2130.
22. K. Wang, M. Q. He, F. H. Zhai, J. Wang, R. H. He and Y. L. Yu, *Biosens. Bioelectron.*, 2018, **105**, 159-165.
23. S. Bi, S. Z. Yue, Q. Wu and J. Y. Ye, *Chem. Commun.*, 2016, **52**, 5455-5458.
24. P. Miao, Y. T. Jiang, T. Zhang, Y. Huang and Y. G. Tang, *Chem. Commun.*, 2018, **54**, 7366-7369.
25. Z. F. Shen, F. Li, Y. F. Jiang, C. Chen, H. Xu, C. C. Li, Z. Yang and Z. S. Wu, *Anal. Chem.*, 2018, **90**, 3335-3340.
26. F. A. Wang, L. Freage, R. Orbach and I. Willner, *Anal. Chem.*, 2013, **85**, 8196-8203.
27. B. C. Yin, Y. Q. Liu and B. C. Ye, *Anal. Chem.*, 2013, **85**, 11487-11493.
28. L. Ge, W. X. Wang, X. M. Sun, T. Hou and F. Li, *Anal. Chem.*, 2016, **88**, 9691-9698.
29. X. J. Qu, H. J. Jin, Y. Q. Liu and Q. J. Sun, *Anal. Chem.*, 2018, **90**, 3482-3489.
30. Z. J. Huang, Z. W. Luo, J. M. Chen, Y. Xu and Y. X. Duan, *ACS Sens.*, 2018, **3**, 2423-2431.
31. P. Miao, K. Han, H. X. Sun, J. Yin, J. Zhao, B. D. Wang and Y. G. Tang, *ACS Appl. Mater. Interfaces*, 2014, **6**, 8667-8672.
32. A. Abi, M. H. Lin, H. Pei, C. H. Fan, E. E. Ferapontova and X. L. Zuo, *ACS Appl. Mater. Interfaces*, 2014, **6**, 8928-8931.
33. X. Zhang, B. W. Liu, M. R. Servos and J. W. Liu, *Langmuir*, 2013, **29**, 6091-6098.
34. G. Braun, S. J. Lee, M. Dante, T. Nguyen, M. Moskovits and N. Reich, *J. Am. Chem. Soc.*, 2007, **129**, 6378-6379.
35. B. W. Liu and J. W. Liu, *Anal. Methods*, 2017, **9**, 2633-2643.
36. F. Xu, H. F. Dong, Y. Cao, H. T. Lu, X. D. Meng, W. H. Dai, X. J. Zhang, K. A. Al-Ghanim and S. Mahboob, *ACS Appl. Mater. Interfaces*, 2016, **8**, 33499-33505.
37. L. Liang, J. Li, Q. Li, Q. Huang, J. Y. Shi, H. Yan and C. H. Fan, *Angew. Chem., Int. Ed.*, 2014, **53**, 7745-7750.
38. H. M. Ding, J. Li, N. Chen, X. J. Hu, X. F. Yang, L. J. Guo, Q. Li, X. L. Zuo, L. H. Wang, Y. Q. Ma and C. H. Fan, *ACS Cent. Sci.*, 2018, **4**, 1344-1351.
39. P. Miao, T. Liu, X. X. Li, L. M. Ning, J. Yin and K. Han, *Biosens. Bioelectron.*, 2013, **49**, 20-24.
40. P. Song, M. Li, J. W. Shen, H. Pei, J. Chao, S. Su, A. Aldalbahi, L. H. Wang, J. Y. Shi, S. P. Song, L. H. Wang, C. H. Fan and X. L. Zuo, *Anal. Chem.*, 2016, **88**, 8043-8049.

View Article Online
DOI: 10.1039/C9TB00274J

View Article Online
DOI: 10.1039/C9TB00274J

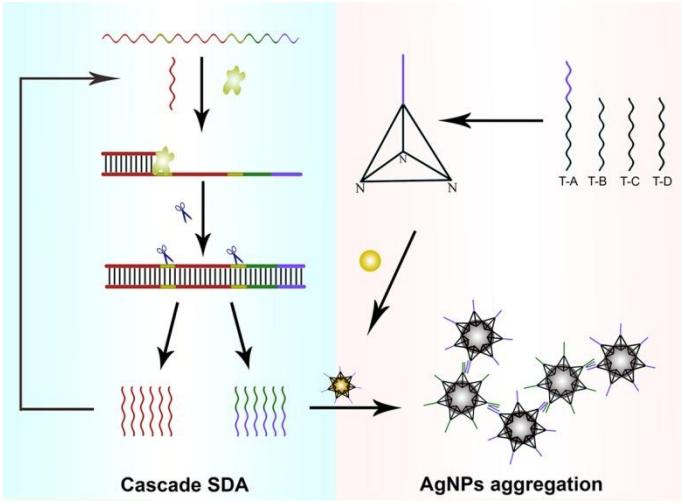

DNA tetrahedrons modified silver nanoparticles are constructed for colorimetric analysis of HIV-related DNA with strand displacement polymerization and nicking endonuclease aided cycles.